General Disclaimer

One or more of the Following Statements may affect this Document

- This document has been reproduced from the best copy furnished by the organizational source. It is being released in the interest of making available as much information as possible.

- This document may contain data, which exceeds the sheet parameters. It was furnished in this condition by the organizational source and is the best copy available.

- This document may contain tone-on-tone or color graphs, charts and/or pictures, which have been reproduced in black and white.

- This document is paginated as submitted by the original source.

- Portions of this document are not fully legible due to the historical nature of some of the material. However, it is the best reproduction available from the original submission.

E-2594

APPROXIMATE OPTIMAL ATMOSPHERIC ENTRY TRAJECTORIES

by

Jason Speyer and Edward Womble

July, 1971

CHARLES STARK DRAPER LABORATORY

MASSACHUSETTS INSTITUTE OF TECHNOLOGY

CAMBRIDGE, MASSACHUSETTS, 02139

E-2594

APPROXIMATE OPTIMAL ATMOSPHERIC ENTRY TRAJECTORIES

by

Jason Speyer and Edward Womble

July, 1971

CHARLES STARK DRAPER LABORATORY
MASSACHUSETTS INSTITUTE OF TECHNOLOGY
CAMBRIDGE, MASSACHUSETTS

Approved: Donald C Fraser Date: 28 July 1971
D. C. FRASER, ASSISTANT DIRECTOR

Approved: R. H. Battin Date: 28 July 71
R. H. BATTIN, ASSOCIATE DIRECTOR

Approved: D. G. Hoag for DGH Date: 28 Jul 71
D. G. HOAG, ASSOCIATE DIRECTOR

Approved: Ralph R. Ragan Date: 28 Jul 71
R. R. RAGAN, DEPUTY DIRECTOR

ACKNOWLEDGEMENT

This report was prepared under DSR Project 55-40800, sponsored by the Manned Spacecraft Center of the National Aeronautics and Space Administration through Contract NAS 9-10268.

To be presented at
The AIAA Guidance, Control and
Flight Mechanics Conference
Stony Brook, New York
August 1971

APPROXIMATE OPTIMAL ATMOSPHERIC ENTRY TRAJECTORIES

Jason L. Speyer* and M. Edward Womble**
Charles Stark Draper Laboratory, M.I.T.
Cambridge, Massachusetts

Abstract

For a re-entry glider, approximate solutions are found in closed form for the problem of maximizing a function of the terminal velocity, altitude, flight path angle and heading angle subject to, at most, three terminal nonlinear constraints. The results given here extend the previous results in two important ways:

1. The second order approximation of the entry dynamics of Loh is used instead of the first order approximation of Allen and Eggers. This approximation is found to compare extremely well with an exact numerical optimal path.
2. A three dimensional optimization problem is solved which includes Loh's second order approximation where the roll angle as well as the lift coefficient are determined subject to constraints which include the terminal heading angle. Furthermore, closed form solutions can also be obtained subject to inflight constraints on the lift coefficient and roll angle.

This work was supported by NASA under contract NAS9-10268.

* Staff

** Graduate Student, research assistant.

The authors would like to thank Ted Edelbaum for many interesting discussions about Loh's work and Michel Froidevaux for his comments on the out-of-plane motion. Part of this work was done by the first author while a consultant at Raytheon Co.

I. Introduction

The problem of optimum lift, drag and roll angle control of a hypersonic lifting body during re-entry is so difficult that most available solutions are numerical.[1] The available analytic solutions of the re-entry equations (no optimization) are quite restrictive being derived under such assumptions as constant lift-to-drag ratio or constant lift and constant drag coefficients. Recently, analytic solutions were obtained for optimal re-entry maneuvers which extremize a function of the terminal attitude, velocity and flight path angle with constraints on any two terminal states.[2,3] These analytic solutions are important because they allow insight into the structure of the optimal control policy and may form the basis for the solution of the guidance problem. The region of validity of the results of Refs. 2 and 3 are greatly extended here and the analytical results are shown to compare favorably with previous numerical solutions. The performance index of most practical concern for which these analytical results apply is that of minimizing total energy loss. This allows efficient energy management for maneuvers - i.e., reversing the heading angle of a shuttle type vehicle so as to be left with sufficient energy to reach a desired landing site. However, this analysis is applicable to a general class of entry problems where nonlinear functions of the terminal state variables characterize both the performance index and constraints.

Busemann, Vinh and Kelley[2] were able to obtain analytical solutions to an optimal re-entry problem in two dimensions by assuming that the aerodynamic forces greatly exceed the gravity force and centrifugal force[4]. By using the flight path angle as the independent variable and by making a clever transformation on the remaining state variables, the motion equations are found to be an explicit function of only the control variable (lift coefficient λ) and the flight path angle γ. Under these circumstances, the Lagrange multipliers are constants along the motion. Furthermore, the functional form of the extremizing control variable (for a parabolic lift-drag polar) is simply

$$\lambda = (1 + p_2 \sin\gamma)^{1/2} \tag{1}$$

where the constant p_2 is found by satisfying the terminal altitude constraint

at a given terminal γ. This necessitates solving an equation involving elliptic integrals. However, if γ is assumed small, the integrals can be evaluated in closed form. Shi[3] extends these results by using the method of matched asymptotic expansions to join the Keplerian region to the region valid for the approximation of Allen and Egger.

These results can be extended without any further assumptions (flat Earth is already assumed) to include the heading angle. This out-of-plane motion is obtained by rolling the vehicle about the velocity vector. In an extended Busemann state space, the vehicle motion depends only on explicit functions of λ, the roll angle μ, and γ; therefore the Lagrange multipliers again are constants along the motion. The functional form of the extremizing roll angle (consistant with a parabolic polar) is

$$\sin\mu = p_1 / 2 \cos\gamma\lambda \qquad (2)$$

where λ is given by (1) and the constant p_1 is found by satisfying the terminal heading angle constraint at a given terminal γ. Both p_1 and p_2 are found by satisfying two equations involving elliptic integrals simultaneously. If γ is assumed small, closed form solutions are obtained.

The Allen and Eggers[4] approximation seems to be valid for high aerodynamic force regions or regions where the flight-path angle is small and the lift-to-drag ratio large and positive.[5] For the two dimensional problem, Loh[5] is able to find valid analytical soutions in a region far larger than that of Ref. 4 by including a second order correction term. This second order term includes some of the affects of gravity and centrifugal force on the trajectory and is included here to extend Busemann's analytic solution (i.e., equations (1) and (2)) to a much wider region of validity for both the two and three dimensional cases. Interestingly the form of the roll angle given in (2) is quite general. However, the form of λ is considerably changed from that of (1). Nevertheless, for small γ closed form solutions can be obtained. For the two dimensional case, this approximation is found to compare quite favorably with a numerically obtained optimum path.

At present only in-flight constraints can be directly imposed upon (λ, μ) if the bounds are constants. This is because along a control variable constraint boundary the Lagrange multipliers still remain constants of the

motion. Although along a roll angle boundary the form of λ is similar to (1), along a λ boundary the form of μ is quite different especially if Loh's second-order term is included.

II. Equations of Motion

The equations of motion in 3-dimensions for a point mass over a spherical non-rotating Earth are

$$\dot{\delta} = V \cos\gamma \cos\psi/(R_0 + h) \sin\theta \tag{3}$$

$$\dot{\theta} = V \sin\psi \cos\gamma (R_0 + h) \tag{4}$$

$$\dot{h} = V \sin\gamma \tag{5}$$

$$\dot{V} = \frac{D}{m} - \frac{g_0 R_0^2}{(R_0 + h)^2} \sin\gamma \tag{6}$$

$$\dot{\gamma} = \frac{L \cos\mu}{mV} + \left(\frac{V}{R_0 + h} - \frac{g_0 R_0^2}{V(R_0 + h)^2}\right) \cos\gamma \tag{7}$$

$$\dot{\psi} = \frac{L \sin\mu}{mV \cos\gamma} - \frac{V}{R_0 + h} \cos\gamma \sin\psi \operatorname{ctn}\theta \tag{8}$$

The coordinate system is illustrated in Fig. 1 where δ is the down range angle, θ is the cross range angle, V is the velocity magnitude, h is the altitude, γ is the flightpath angle, ψ is the heading angle, μ is the roll angle, R_0 is radius of the Earth, m is the vehicle mass, g_0 is the gravitational acceleration at sea level, and L and D are the lift and drag forces given as

$$L = \rho V^2 S C_L/2 \tag{9}$$

$$D = \rho V^2 S C_D/2 \tag{10}$$

where S is the surface area, ρ is the density assumed to be exponential as

$$\rho = \rho_0 e^{-h/\beta} \tag{11}$$

where ρ_0 is the density at sea level and β is the scale height. The drag coefficient C_D is assumed to be only functional related to the lift coefficient C_L, the control variable.

III. Approximation of Equations of Motion

In the first order approximation of Allen and Eggers[4], the assumption that the aerodynamics forces are dominant is equivalent to considering a flat earth with no gravity force. However, in certain regions of interest large errors may occur. Loh's[5] second order approximation includes some of the effects of the centrifugal (spherical Earth) and gravitational forces in an attempt to expand the region of validity of the approximation of Ref. 4. Let us rewrite (7) as

$$\frac{d\gamma}{dt} = \rho V \left[\frac{C_L S \cos \mu}{2m} + M \right] \tag{12}$$

where

$$M = \left[1 - g_0 R_0^2 / V^2 \, (R_0 + h) \right] \cos \gamma / \rho \, (R_0 + h) \tag{13}$$

Loh accounts for the gravity and centrifugal force in the $\dot{\gamma}$ equation by observing from numerical simulations that M is insensitive to integration with respect to ρ or γ and thereby can be treated as a constant (the Busemann scheme, to be described subsequently, uses γ as the variable of integration). Loh's approximation is substantiated by the excellent agreement he obtains between the approximate and exact numerical solution. Loh's approximation extended to the 3 dimensional problem is

1. M is insensitive to γ integration and therefore assumed constant.
2. $g \sin \gamma \ll D/m$ and therefore neglected.
3. $V/(R_0 + h) \cos \gamma \sin \psi \operatorname{ctn} \theta \ll 1$ and thereby neglected.

For small flight path angle approximations (which will be typically the case for manned maneuvers) approximation 2 seems to be reasonably valid. If large cross ranges are not covered (θ small) approximation 3 seems to be

valid. Reference 6 presents numerical evidence on conditions when approximation 3 gives good accuracy even though the lateral range is large.

The equations of motion (5-8) using the above approximations become

$$\dot{V} = -C_D V^2 S/2m \tag{14}$$

$$\dot{\gamma} = \rho V[(C_L S \cos\mu)/2m + M] \tag{15}$$

$$\dot{h} = V \sin\gamma \tag{16}$$

$$\dot{\psi} = \frac{\rho V C_L S \sin\mu}{2m \cos\gamma} \tag{17}$$

The down range and cross range angles are not included in the following analysis and by approximation 3 are not included in the above equations of motion.

IV. Transformation of State Variables

If the independent variable is changed using (15) from t to γ and if the transformation

$$\eta = h/\beta \quad , \quad w = \frac{\rho_0 \beta C_L^* S e^{-\eta}}{2m} \tag{18}$$

$$u = 2 \frac{C_L^*}{C_D^*} \ln[V/(\beta g)^{1/2}] \tag{19}$$

given in Ref. 2 is used where w is a dimensionless altitude, u is a dimensionless velocity, and C_L^* and C_D^* are constants defined in Section 5.1, the equations of motion, (14) - (17) become

$$du/d\gamma = -2(C_D/C_D^*)/[(C_L/C_L^*)\cos\mu + \underline{M}] \tag{20}$$

$$dw/d\gamma = -\sin\gamma/[(C_L/C_L^*)\cos\mu + \underline{M}] \tag{21}$$

$$d\psi/d\gamma = (C_L/C_L^*)\sin\mu/[(C_L/C_L^*)\cos\mu + \underline{M}]\cos\gamma \tag{22}$$

where

$$\underline{M} = 2m\ M/C_L^* S \tag{23}$$

Note that these equations are only explicit functions of the controls (C_L, μ) and the independent variable, γ. This has important consequences in obtaining a closed form solution to the optimization problem. Note that γ is not monotonic and care must be taken at a point of inflection, i.e. a point where $\dot{\gamma}$ changes sign.

V. The Optimal Control Problem

In general the problem is to find the control histories (C_L, μ) over the interval $\gamma \in [\gamma_0, \gamma_f]$ which maximize the terminal function $\phi[u(\gamma_f), w(\gamma_f), \psi(\gamma_f), \gamma_f]$ subject to the dynamics (20 - 22) with specific initial conditions, the terminal constraints

$$\Omega[u(\gamma_f), w(\gamma_f), \psi(\gamma_f), \gamma_f] = 0 \tag{24}$$

where Ω is at most a column three vector of constraint functions, and the control inequality constraints

$$C_L^{min} \le C_L \le C_L^{max}, \quad \mu^{min} \le \mu \le \mu^{max} \tag{25}$$

In the above γ_0 and γ_f are the initial and final values of γ.

Define the variational Hamiltonian as

$$H = [p_1 (C_L/C_L^*) \sin\mu/\cos\gamma - p_2 \sin\gamma - 2p_3 (C_D/C_D^*)]/[(C_L/C_L^*)\cos\mu + \underline{M}] \tag{26}$$

and an augmented terminal function as

$$\Phi = \phi + \nu\,\Omega \tag{26a}$$

where the Lagrange multipliers (p_1, p_2, p_3) are associated with the differential constraints (22), (21), (20), respectively. The Lagrange multiplier row vector ν is associated with the terminal constraints (24).

The Euler-Lagrange equations are

$$dp_1/d\gamma = -\partial H/\partial \psi = 0, \qquad dp_2/d\gamma = -\partial H/\partial w = 0,$$

$$dp_3/d\gamma = -\partial H/\partial u = 0 \tag{27}$$

with terminal transversality conditions

$$p_1(\gamma_f) = \partial \Phi/\partial \psi\Big|_{\gamma=\gamma_f}, \qquad p_2(\gamma_f) = \partial \Phi/\partial w\Big|_{\gamma=\gamma_f}$$

$$p_3(\gamma_f) = \partial \Phi/\partial u\Big|_{\gamma=\gamma_f}, \qquad H(\gamma_f) = \partial \Phi/\partial \gamma\Big|_{\gamma=\gamma_f} \tag{28}$$

Clearly, the advantage of the transformation of Ref. 2 is that the multiplier dynamics are zero; the Lagrange multipliers are constant along the motion.

The optimality conditions applicable when the control variables lie in the interior of the admissible control set are

$$\partial H/\partial C_L = 0, \qquad \partial H/\partial \cos\mu = 0 \tag{29}$$

which reduce to

$$\frac{p_1 \sin\mu}{\cos\gamma} + p_2 \sin\gamma \cos\mu + 2p_3 \left[(C_D/C_D^*) \cos\mu - \frac{C_L}{C_D^*} \frac{\partial C_D}{\partial C_L} \cos\mu - \frac{\partial C_D}{\partial C_L} \frac{C_L^*}{C_D^*} \underline{M} \right] = 0 \tag{30}$$

$$-\frac{p_1}{\cos\gamma} \frac{\cos\mu\, \underline{M} + (C_L/C_L^*)}{\sin\mu} + p_2 \sin\gamma + 2p_3 C_D/C_D^* = 0 \tag{31}$$

respectively.

These conditions can be simplified. If (31) multiplied by $\cos\mu$ is subtracted from (30), the result is

$$\sin\mu = p_1/[2p_3 \cos\gamma (\partial C_D/\partial C_L)(C_L^*/C_D^*)] \tag{32}$$

This general result relates the roll angle to the slope of the lift-drag polar. It is assumed that p_3 is not zero. If p_3 is zero the Lagendre-Clebsch

condition[1] cannot be satisfied. If (32) is substituted into (30), we have

$$\pm \underline{M} \{[2 \cos\gamma \, (\partial C_D/\partial C_L)(C_L^*/C_D) \, p_3]^2 - p_1^2\}^{1/2}/\cos\gamma$$

$$= p_2 \sin\gamma + 2p_3[C_D - C_L(\partial C_D/\partial C_L)]/C_D^* \qquad (33)$$

Note that the multipliers can be normalized in both (32) and (33) by defining two constants $\underline{p}_1 \triangleq p_1/p_3$ and $\underline{p}_2 \triangleq p_2/p_3$. The functional dependence between C_L and C_D must be given explicitly. While a general Newtonian polar has been found too complex, an elliptic polar was successfully carried through all the analysis.[7] A simpler form will be used in the following analysis.

5.1 Optimal lift coefficient for parabolic lift-drag polar

In Ref. 2 the form of the lift-drag polar is

$$C_D = C_{D_0} + K C_L^n \quad ; \quad n > 1 \qquad (34)$$

where C_{D_0} and K are constants. The analysis to follow can be carried out for arbitrary n; however, for notational convenience we consider a parabolic polar (n = 2). For consistency with Ref. 2 the control variable used is a quasi lift coefficient λ defined as

$$\lambda^2 = K C_L^2/C_{D_0} \qquad (35)$$

The lift and drag coefficients are related to λ as

$$C_L = C_L^* \lambda \quad , \quad C_D = \frac{1}{2} C_D^*(1 + \lambda^2) \qquad (36)$$

where

$$C_L^* = (C_{D_0}/K)^{1/2} \quad , \quad C_D^* = 2 C_{D_0} \qquad (37)$$

C_L^* and C_D^* are the lift and drag coefficients corresponding to the maximum lift to drag ratio.

Using the above parabolic polar, (33) becomes

$$\pm \underline{M}\,[4\cos^2\gamma\lambda^2 - \underline{p}_1^2]^{1/2}/\cos\gamma = \underline{p}_2 \sin\gamma + [1 - \lambda^2] \tag{38}$$

from which λ^2 can be found as

$$\lambda^2 = (2\,\underline{M}^2 + \underline{p}_2 \sin\gamma + 1)$$

$$\pm 2\,\underline{M}\,(\underline{M}^2 + \underline{p}_2 \sin\gamma + 1 - \underline{p}_1^2/4\cos^2\gamma)^{1/2} \tag{39}$$

The above can be put into a more useful and elegant form if the term $p_1/4\cos^2\gamma$ is added and subtracted from (39) as

$$\lambda = [(-\underline{M} \pm \ell^{1/2})^2 + \underline{p}_1^2/4\cos^2\gamma]^{1/2} \tag{40}$$

where ℓ is defined as

$$\ell = \underline{M}^2 + \underline{p}_2 \sin\gamma + 1 - \underline{p}_1^2/4\cos^2\gamma \tag{41}$$

Furthermore, (45) using a parabolic polar reduces to

$$\sin\mu = \underline{p}_1/2\cos\gamma\lambda \tag{42}$$

The analytic form of the optimal (λ, μ) are given in (40) and (42) in terms of only two constants $\underline{p}_1$ and $\underline{p}_2$. Evaluation of these constants will be discussed in the next section along with the plus or minus sign ($\pm$) in (40).

Notice that $\sin\mu$ in (42) is inversely proportional to λ. This means λ cannot go through zero unless $\underline{p}_1$ is zero. In fact, λ reaches its lowest value of $\underline{p}_1/2\cos\gamma$ when $\ell^{1/2} = \underline{M}$ which occurs when $\mu = \pm 90^\circ$. λ is considered to only modulate the magnitude of the lift and is assumed always positive whereas the direction of lift is completely determined by the roll angle.

5.2 Evaluation of the Lagrange multipliers

The constants $\underline{p}_1$ and $\underline{p}_2$ are evaluated by satisfying the terminal condition (24) and transversality conditions (28) which are evaluated by determining the terminal state variables as a function of these constants.

By introducing (40) and (42) into (20 - 22) and integrating we obtain the terminal values of u, w, and ψ at $\gamma = \gamma_f$. These seemingly complicated integrals can be greatly reduced by the following algebraic manipulations and observations. From (42)

$$\cos^2\mu = 1 - \sin^2\mu = [\lambda^2 - \underline{p}_1^2/4 \cos^2\gamma]/\lambda^2 \tag{43}$$

Using (43) and (40) the denominator of (20 - 22) reduces to

$$\lambda \cos\mu + \underline{M} = \pm[\lambda^2 - \underline{p}_1^2/4 \cos^2\gamma]^{1/2} + \underline{M} = \pm \iota^{1/2} \tag{44}$$

However, this reduction is not obvious because of the sign indeterminacies found in λ and $\cos\mu$. This difficulty is overcome by noting that in the limit as $\underline{p}_1$ goes to zero, (40) must reduce to the two dimensional case found from the optimality condition (30) where $\underline{p}_1 = 0$ and $\mu = 0$, i.e.

$$\lambda = -\underline{M} \pm(\underline{M}^2 + 1 + \underline{p}_2 \sin\gamma)^{1/2} \tag{45}$$

The form of (40) and (44) are chosen to be consistant with (45) and $\lambda + \underline{M}$ respectively, as the limit of the two dimensional case is approached.

The sign of $\iota^{1/2}$ in (44) indicates whether $\dot{\gamma}$ is positive or negative. Then if ι goes through zero, an inflection point of γ is reached (γ attains an extreme value). At this point the sign of $\iota^{1/2}$ changes. In the following integrals, the interval of integration is divided at the inflection point of γ, γ_I. Note γ_I is found by setting ι equal to zero in (41). It is conjectured that at most only one inflection point will occur.

Introducing (44) into (20 - 22) the following integrals result

$$u(\gamma_f) - u(\gamma_0) = 2\underline{M}(\gamma_f - \gamma_0) \mp \int_{\gamma_0}^{\gamma_I} \pm \int_{\gamma_I}^{\gamma_f} d\gamma\,[1 + \underline{M}^2 + \iota + \underline{p}_1^2/4 \cos\gamma]/\iota^{1/2} \tag{46}$$

$$w(\gamma_f) - w(\gamma_0) = \mp \int_{\gamma_0}^{\gamma_I} \pm \int_{\gamma_I}^{\gamma_f} d\gamma \sin\gamma/\iota^{1/2} \tag{47}$$

$$\psi(\gamma_f) - \psi(\gamma_0) = \pm \int_{\gamma_0}^{\gamma_I} \mp \int_{\gamma_i}^{\gamma_f} d\gamma\,(\underline{p}_1/2 \cos^2\gamma\, \iota^{1/2}) \tag{48}$$

These integrals reduce to, at best, elliptic integrals which are however, tabulated. If the flight path angle is assumed small ($\cos\gamma \sim 1$, $\sin\gamma \sim \gamma$), (46 - 48) can be integrated in closed form as

$$u(\gamma_f) - u(\gamma_0) = \mp\frac{2}{\underline{p}_2}\Big[\{a[\underline{p}_2\gamma_f + b]^{1/2} + \frac{1}{3}[\underline{p}_2\gamma_f + b]^{3/2}\}$$

$$\pm\{a[\underline{p}_2\gamma_0 + b]^{1/2} + \frac{1}{3}[\underline{p}_2\gamma_0 + b]^{3/2}\}\Big] + 2\underline{M}(\gamma_f - \gamma_0) \qquad (49)$$

$$w(\gamma_f) - w(\gamma_0) = \mp\{[2\underline{p}_2\gamma_f - 4b][\underline{p}_2\gamma_f + b]^{1/2}/3\,\underline{p}_2^2$$

$$\pm[2\underline{p}_2\gamma_0 - 4b][\underline{p}_2\gamma_0 + b]^{1/2}/3\,\underline{p}_2^2\}\,, \qquad (50)$$

$$\psi(\gamma_f) - \psi(\gamma_0) = \pm(\underline{p}_1/\underline{p}_2)\{[\underline{p}_2\gamma_f + b]^{1/2}$$

$$\pm[\underline{p}_2\gamma_0 + b]^{1/2}\} \qquad (51)$$

where

$$a = \underline{M}^2 + 1 + \underline{p}_1^2/4\,, \qquad b = \underline{M}^2 + 1 - \underline{p}_1^2/4 \qquad (52)$$

The $\pm$ sign in front of the entire expression of the right hand side of (49 - 51) indicates whether γ is increasing or decreasing at γ_f. The $\pm$ sign multiplying the second term in (49 - 51) indicates whether or not an inflection point exists. The minus sign means there is no inflection point whereas a plus sign means an inflection point does exist. The four possible combinations of signs may lead to four different real values of the constant p_1, p_2, p_3, and γ_f for which the terminal boundary conditions given by the constraints (24) and the transversality conditions (28) are satisfied. The terminal conditions are written in terms of the constants by eliminating the terminal state variables through (49 - 51) and using the equations of (28) to eliminate the ν's. In this way four nonlinear conditions are to be satisfied by the

four constants p_1, p_2, p_3 and γ_f. Note that, in general, $p_3 \neq 0$ can be eliminated by normalizing p_1 and p_2; thereby, only three constants ($\underline{p}_1$, $\underline{p}_2$, γ_f) need be found. This, in general, requires a numerical procedure but only nonlinear algebraic equations are involved and not nonlinear differential equations. Although four different solutions may give real values for the constants, only one solution will be the global maximum. The other solutions if they exist will be either local maximum or extremal paths which do not satisfy second order necessary conditions, i.e. Legendre-Clebsch condition or the Jacobi (conjugate point) test[1] fail. The global maximum gives the best value of ϕ from all possible solutions.

VI. Comments on Results

Let us specialize the preceding results to the problem of maximizing the terminal velocity (minimum energy loss) subject to terminal constraints on the altitude, flight path angle and heading angle. Since $p_3 = 1$ for maximum terminal velocity and γ_f are given, only p_1 and p_2 need be found from (50) and (51). Once these constants are obtained, the optimal control programs are obtained by (40) and (42) and the normalized terminal velocity is given by (46). In a second example of interest the terminal heading angle and flight path angle are specified, the terminal altitude is free, and the total terminal energy ($V^2 + 2 g_0 h$) is to be maximized. In this case the multipliers can be normalized with $\underline{p}_3 = 1$. The $\underline{p}_1$ and $\underline{p}_2$ are found so that (51) and the transversality condition $\underline{p}_2 = -g_0/V^2\rho \triangleq r(\underline{p}_1, \underline{p}_2)$ are satisfied. The function r is obtained by characterizing $V(\gamma_f)$ and $h(\gamma_f)$ in terms of $\underline{p}_1$ and $\underline{p}_2$ through (49) and (50).

As was noted the form of the roll angle is very general and is dependent on a particular approximation only through its dependence on λ. However, for the first (M = 0) and second (Loh) order approximations, the form of λ changes considerably. The general form is given in (40) and reduces to (45) for the 2-dimensional case and for both the 2- and 3-dimensional cases to

$$\lambda = \pm (1 + p_2 \sin\gamma)^{1/2} \tag{53}$$

for the first order approximation. This is the form found in Ref. 2. In

(53) λ changes sign at the inflection point of γ. The effect of M is to separate the points where the inflection point occurs and λ goes through zero and to include the effect of p_1 on λ. Similar results for the three dimensional case although with M = 0 were independently obtained by Griffin.[8]

VII. Bounded Control

Bounds can be imposed on the control variables (λ, μ) without excessive complication to the approximation. This is because control variable constraints allow the Lagrange multipliers to remain as constants of the motion even along the control boundary. This is true if the constraint boundaries are constants and not functions of time. However, if the roll angle lies on its bound, the lift coefficient λ determined from (30) alone using a parabolic polar is

$$\lambda = -\underline{M}/\cos\mu_B \pm \left(\frac{\underline{M}^2}{\cos^2\mu_B} + 1 + \underline{p}_2 \sin\gamma + \underline{p}_1 \tan\mu_B \underline{M}/\cos\gamma\right)^{1/2} \tag{54}$$

where μ_B is μ on its bound. If λ is inserted into (20 - 22) equations quite similar to (46 - 48) result. If γ is assumed small, the equations can be integrated in closed form resulting in solutions similar to (49 - 51). The constants p_1, p_2, p_3, γ_f are determined so that the sum over constrained and unconstrained arcs satisfy the terminal conditions (24) and (28). This is demonstrated in Ref. 2 for the case where $\underline{M}$ and μ are zero. Note that if $\underline{M}$ is zero μ is not a function of p_1 and thereby the terminal values of h, γ, ψ cannot be satisfied simultaneously.

If C_L lies on its bound, the roll angle control determined from (31) alone is

$$\cos\mu = \left(-\underline{M}\, C_{LB} \pm A[A^2 + \underline{M}^2 - C_{LB}{}^2]^{1/2}\right)/\left(\underline{M}^2 + A^2\right) \tag{55}$$

where

$$A = [\underline{p}_2 \sin\gamma + 2C_{DB}]\cos\gamma/\underline{p}_1 \tag{56}$$

and where C_{LB} is C_L/C_L^* on its bound and C_{DB} is C_D/C_D^* when on a C_L bound. If $\cos\mu$ is substituted into (20 - 22), the resulting integrals for γ

small are quite complicated. However, these integrals can be simplified if the roll angle is used as the independent variable instead of flight path angle. To do this two changes of variables are made. First the differential relation between γ and A obtained from (55) is (γ is assumed small)

$$d\gamma = \underline{p}_1 \, dA/\underline{p}_2 \tag{57}$$

Furthermore, by using (31) and the definition of A in (56), A is related to μ as

$$A = [\cos\mu \, \underline{M} + C_{LB}]/\sin\mu \tag{58}$$

From the differential relation between A and μ obtained from (58) and using (57) we obtain

$$d\gamma = -[\underline{p}_1(C_{LB}\cos\mu + \underline{M})/\underline{p}_2 \sin^2\mu \,] d\mu \tag{59}$$

If γ is eliminated in (20 - 22) by μ using (56), (58) and (59), the equations of motion become simply

$$du/d\mu = 2\underline{p}_1 \, C_{DB}/\underline{p}_2 \sin^2\mu \tag{60}$$

$$dw/d\mu = \underline{p}_1^2(\cos\mu\underline{M} + C_{LB})/\underline{p}_2^2 \sin^3\mu - 2\underline{p}_1 \, C_{DB}/\underline{p}_2^2\sin^2\mu \tag{61}$$

$$d\psi/d\mu = -C_{LB} \, \underline{p}_1 \csc\mu/\underline{p}_2 \tag{62}$$

These equations are easily integrated in closed form. For the case of no inflection point we have

$$u(\gamma_f) - u(\gamma_0) = -2(\underline{p}_1/\underline{p}_2) \, C_{DB}[C(A)/S(A)] \Big|_{A(\gamma_0)}^{A(\gamma_f)} = f^1(\gamma)\Big|_{\gamma_0}^{\gamma_f} \tag{63}$$

$$w(\gamma_f) - w(\gamma_0) = (\underline{p}_1/2\underline{p}_2) \{\underline{p}_1 \, C_{LB} \ln [S(A)/(1 + C(A)]$$

$$- \underline{p}_1 [\underline{M} + C_{LB}C(A)]/[S(A)]^2 + 4 \, C_{DB}C(A)/S(A)\} \Big|_{A(\gamma_0)}^{A(\gamma_f)} = f^2(\gamma)\Big|_{\gamma_0}^{\gamma_f} \tag{64}$$

$$\psi(\gamma_f) - \psi(\gamma_0) = -C_{LB}(p_1/p_2) \ln \{S(A)/[1 + C(A)]\}_{A(\gamma_0)}^{A(\gamma_f)} = f^3(\gamma)\Big|_{\gamma_0}^{\gamma_f} \quad (65)$$

where $C(A) \triangleq \cos\mu$ given by (55) and

$$S(A) \triangleq \sin\mu = [A\, C_{LB} \pm \underline{M}\,(A^2 + \underline{M}^2 - C_{LB}^2)^{1/2}]/(\underline{M}^2 + A^2) \quad (66)$$

An inflection point occurs when the argument of the square root in (55) and (66) goes to zero. That is when

$$A^2(\gamma_1) = C_{LB}^2 - \underline{M}^2 \quad (67)$$

where γ_I is the value of γ at the inflection point easily calculated from (56) and (67). If an inflection point exists the motion equations (60 - 62) result in

$$[u(\gamma_f) - u(\gamma_0),\ w(\gamma_f) - w(\gamma_0),\ \psi(\gamma_f) - \psi(\gamma_0)]$$

$$= \{2\, f^i(\gamma_I) - [f^i(\gamma_f) + f^i(\gamma_0)],\quad i = 1, 2, 3\} \quad (68)$$

where $f^i(\gamma)$ is defined in (63 - 65). Note again that there are four possible solutions. The constants (p_1, p_2, p_3, γ_f) can be found so that the sum over the constrained and unconstrained arcs satisfy the terminal constraints (24) and transversality conditions (28). The control variable is continuous at the junction of constrained and unconstrained arcs.

VIII. Numerical Results

An approximate optimal path, generated using Loh's approximation and assuming that γ is a small angle, is compared to the exact optimal path calculated by a second order numerical optimization technique, the sweep method.[1] The problem is to maximize the terminal velocity subject

to terminal constraints on altitude and flight path angle. The equations of motion used to obtain the exact optimum are given by (5), (6) and (7) with $\mu = 0$. The wing loading, mg/S, was taken as 61.3 lb - ft^2. The 1956 ARDC standard atmosphere model was used for the numerical path and fitted in the region of interest as .0018392 EXP $-(3.978197 \times 10^{-5}h)$ for the approximating path. The lift-drag characteristics of the glider, shown in Fig. 2, are used in both the numerical and approximate path.* The initial conditions for the maximum terminal velocity path were taken as: V = 33,961 ft/sec, $\gamma = -1.57$ deg and h = 189, 890 ft. The terminal constraints are h = 220, 000 ft and $\gamma = 0$.

The approximate optimum solution was calculated using an update method to include the effects of variations in $\underline{M}$ by re-evaluating $\underline{M}$ along the approximate optimal path at given intervals of γ and then adjusting the parameter p_2. It is surprising that the approximation is so good given the variation of $\underline{M}$ with velocity shown in Fig. 3. In Fig. 4 the angle-of-attack program calculated using the above update method (dotted line) is compared with the angle of attack obtained using only the initial value of $\underline{M}$ (dashed line), $\underline{M} = 0$ (dash-dot line), and the exact optimal path (solid line). The path obtained by the update method matches closely with the exact optimum; whereas, when only evaluating $\underline{M}$ initially, the angle of attack of the approximate optimal diverges from the optimum near the terminal point. The effect of making $\underline{M} = 0$ is to increase the angle of attack program. Note that the existence of an inflection point for γ adds no additional complexity in the approximation.

In Fig. 5 the angle of attack program found by using the update method and using $\underline{M} = 0$ is compared with the exact optimum as a function of velocity. Here, the control using the update method differes slightly from the exact control near the inflection point for γ. However, the angle of attack for $\underline{M} = 0$ is considerably different everywhere. In Fig. 6 and 7, the altitude and flight path angle are plotted against velocity showing how close the approximate path (using the update method) is to the exact path in state space. The paths generated by $\underline{M} = 0$ are quite different except at the extremes.

---

* If the angle of attack, α, is related to C_L as $C_L = C_{L_0}\alpha$, then $\lambda = (C_{L_0}/C_L^*)\alpha$ where C_L^* is defined in eq. (37).

The difference in the terminal velocity from the exact path is about -20 ft/sec for the update method and +80 ft/sec for the $\underline{M}$ = 0 approximation.

IX. Conclusions

For a re-entry glider over a spherical non-rotating Earth approximate but closed form solutions are determined for the problem of maximizing a terminal function of the velocity, the heading angle, flight path angle and altitude subject to terminal constraints on these state variable and inflight constraints on the lift coefficient and roll angle. The work here extends Ref. 2 by including Loh's ad hoc second order term and generalizing the problem to three dimensions. These generalizations are made with little additional complexity in those cases where the small flight path angle approximation is justified.

In two dimensions, the approximation of Ref. 2, the extension of Ref. 2 to include Loh's second order term, and a numerical optimum path are compared. The results show that when Loh's term is included the approximate path practically duplicates the numerical path. This is a great improvement over the approximation of Ref. 2. Some additional numerical work done in Ref. 9 for roll modulation only indicates that the three dimensional approximation is also quite good.

References

1. Bryson, A.E., and Ho, Y.C. Applied Optimal Control, Blaisdell, 1969.

2. Busemann, A., Vinh, N.X., and Kelley, G.F., "Optimum Maneuvers of a Skip Vehicle with Bounded Lift Constraints", Journal of Optimization Theory and Applications, Volume 3, Nov. 1969.

3. Shi, Y., "Matched Asymptotic Solutions for Optimum Lift Controlled Atmospheric Entry", presented at the AIAA Guidance Control and Flight Mechancis Conference, August 17-19, 1970.

4. Allen, H.J., and Eggers, A.J., "A Study of the Motion and Aerodynamics Heating of Missile Entering the Earth's Atmosphere at High Supersonic Speeds", NACA Rep. 1381, 1958.

5. Loh, W.H.T., "Entry Mechanics and Dynamics" in Re-entry and Planetary Entry Physics and Technology, edited by W.H.T. Loh, Springer-Verlag Inc., New York, 1968.

6. London, Howard S., "Comment on Lateral Range During Equilibrium Glide" J. Aerospace Science, Vol. 29. No. 5, Jan. 1962.

7. Speyer, J., "Elliptic Lift-Drag Polars", MIT Draper Lab SSV Memo No. 71-23C-2, Dec. 19, 1970.

8. Griffin, J. W. "An Analytical Study of Optimum Three Dimensional Hypervelocity Re-entry Trajectories, "BXA Report 70-210-135, Bendix Aerospace Systems Division, The Bendix Corporation, Ann Arbor, Michigan, Spring, 1970.

9. Speyer, J. and Froidevaux, M., "Approximate Optimal Re-entry Trajectory Using Roll Angle Only", MIT Draper Lab SSV Memo No. 71-23C-5, June 10, 1971.

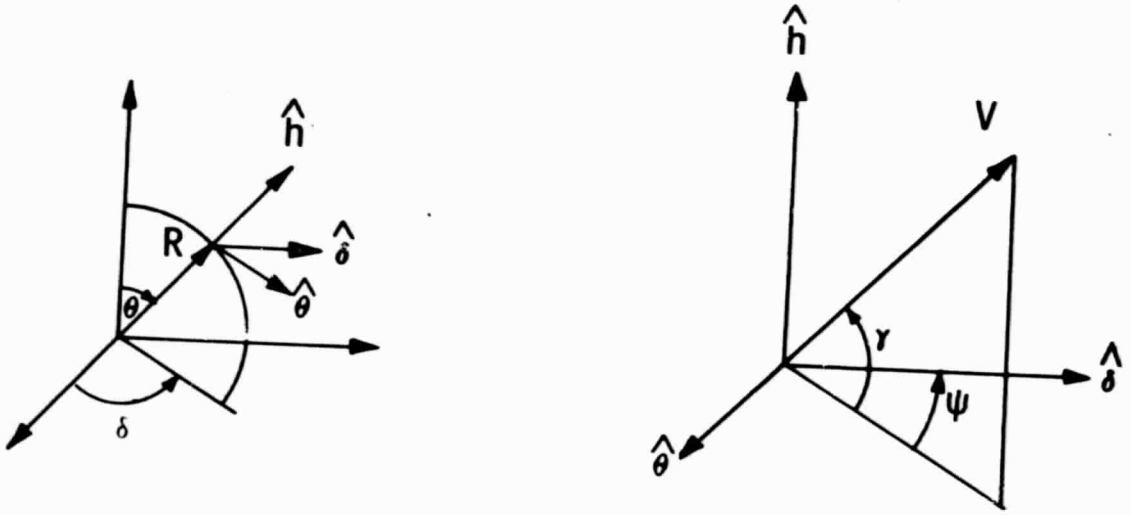

Figure 1. Coordinate System

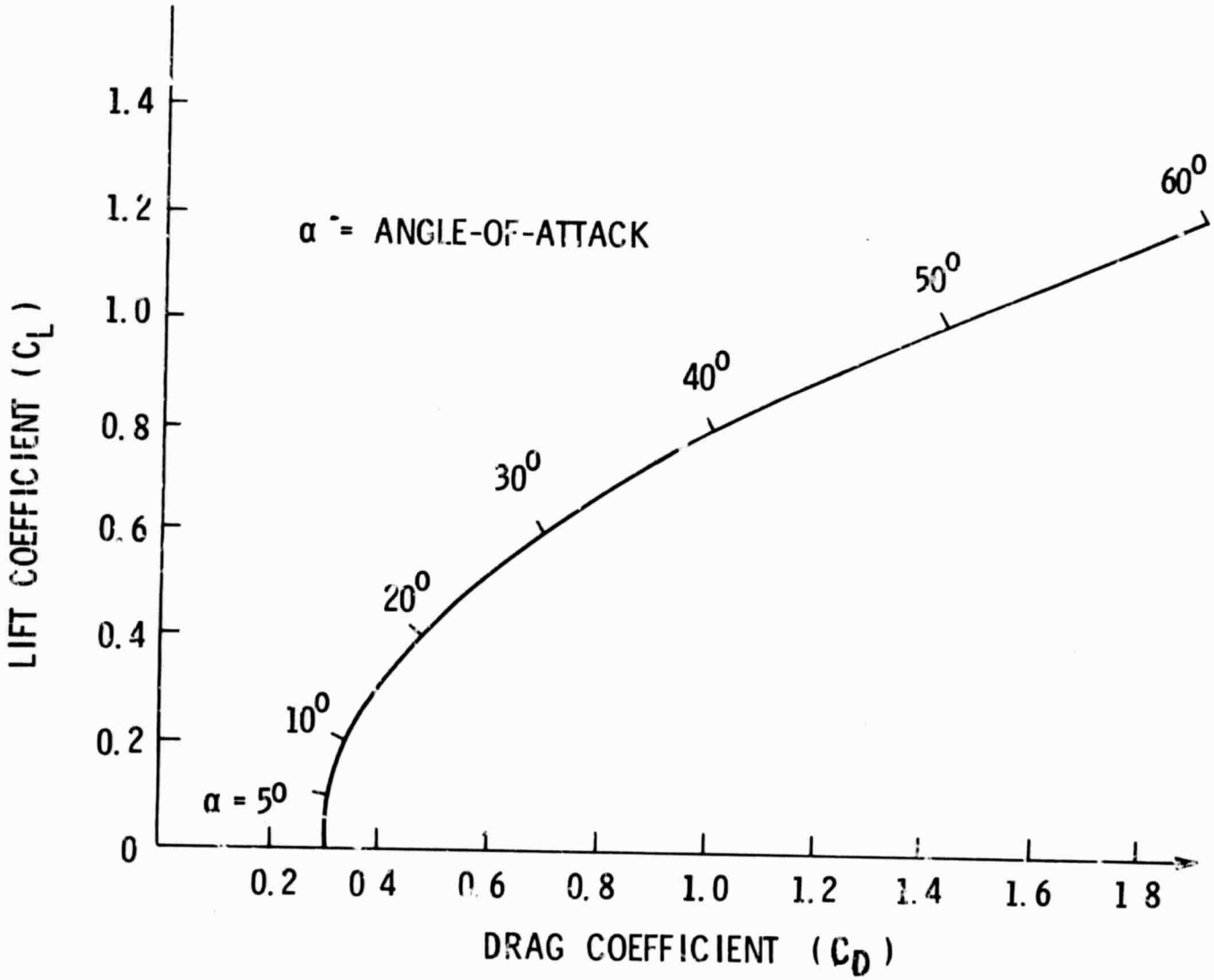

Figure 2 Lift-Drag Polar for Re-Entry Vehicle

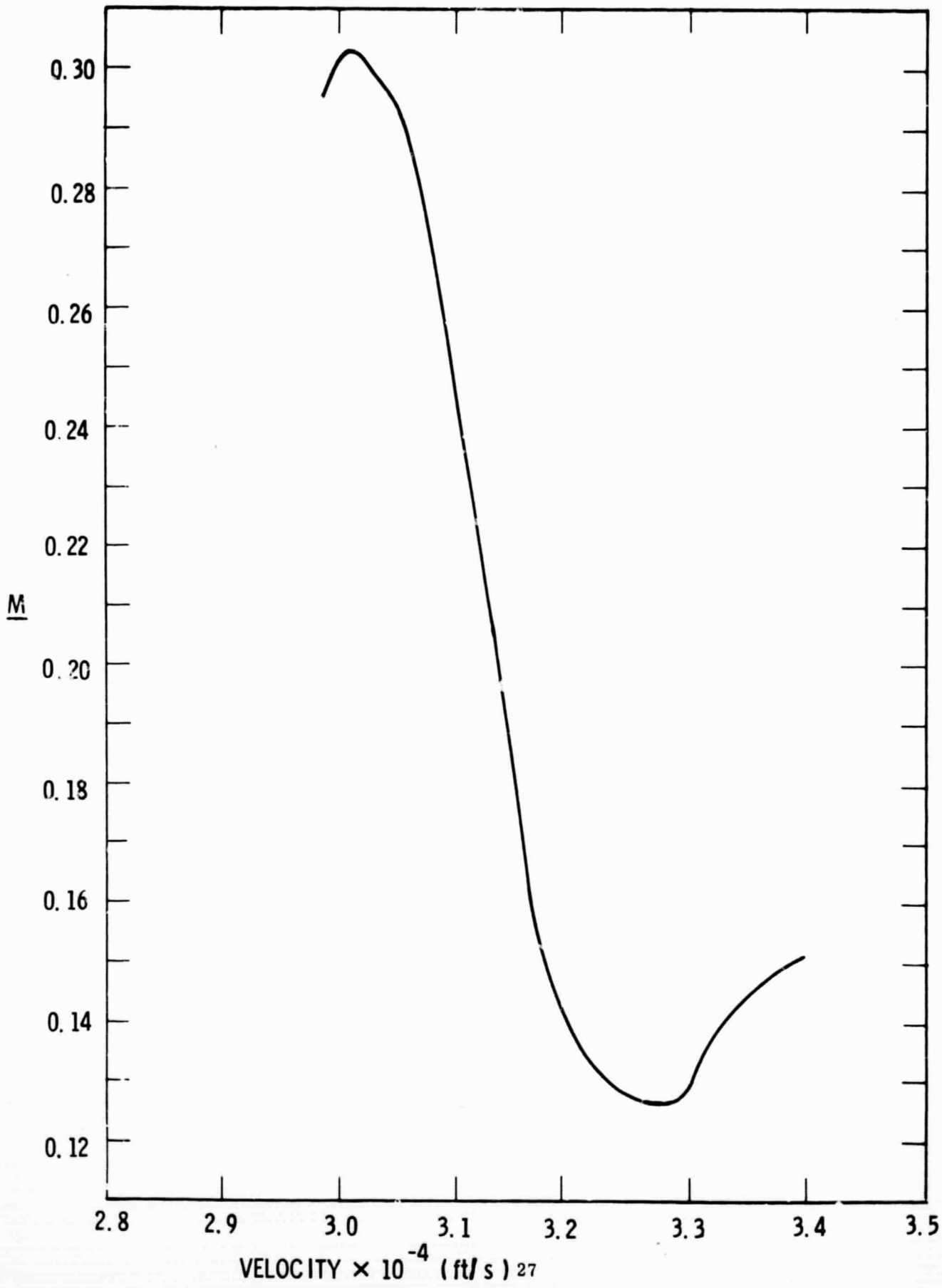

Figure 3 M Versus Velocity

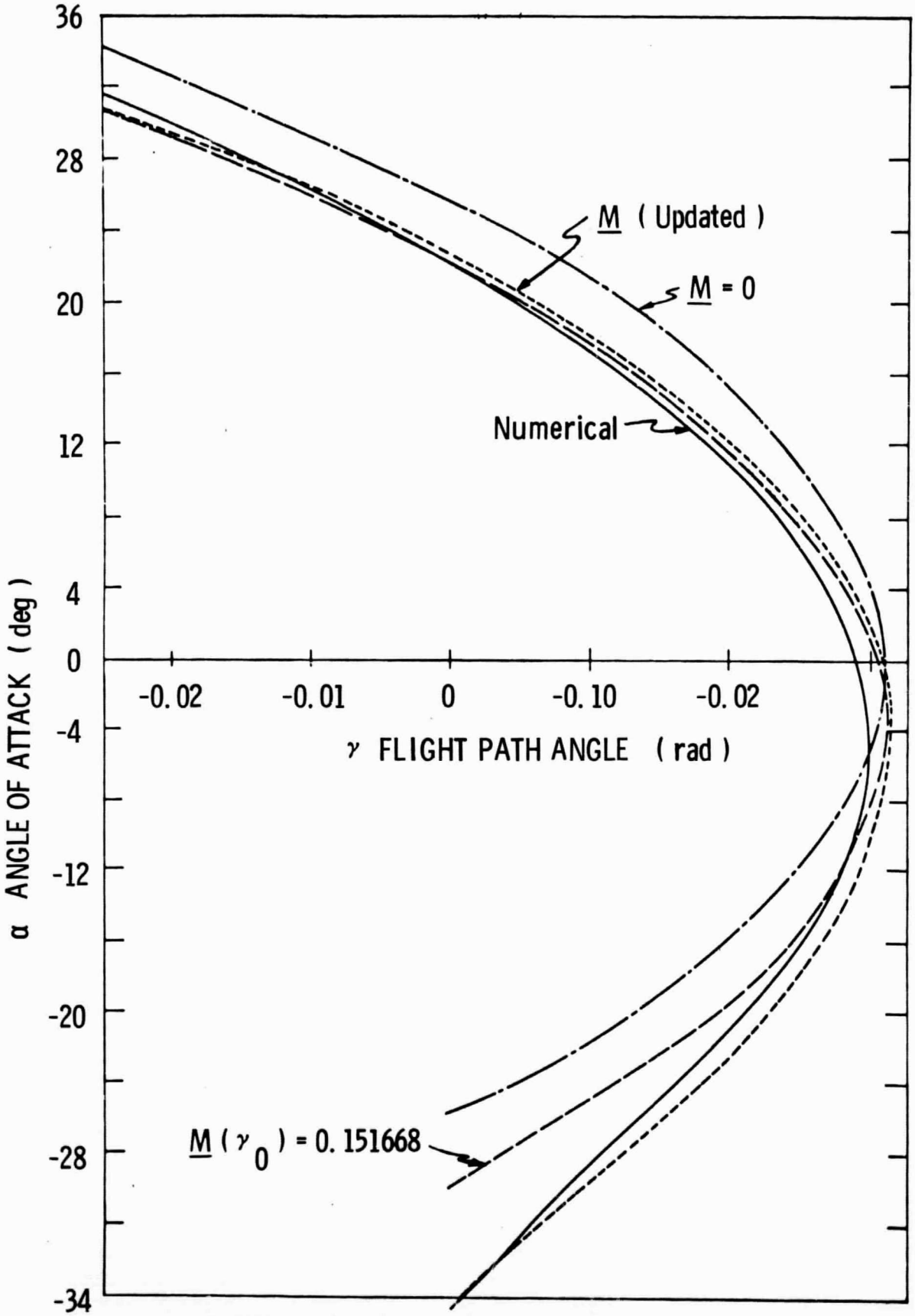

Figure 4 Angle of Attack Versus Flight Path Angle

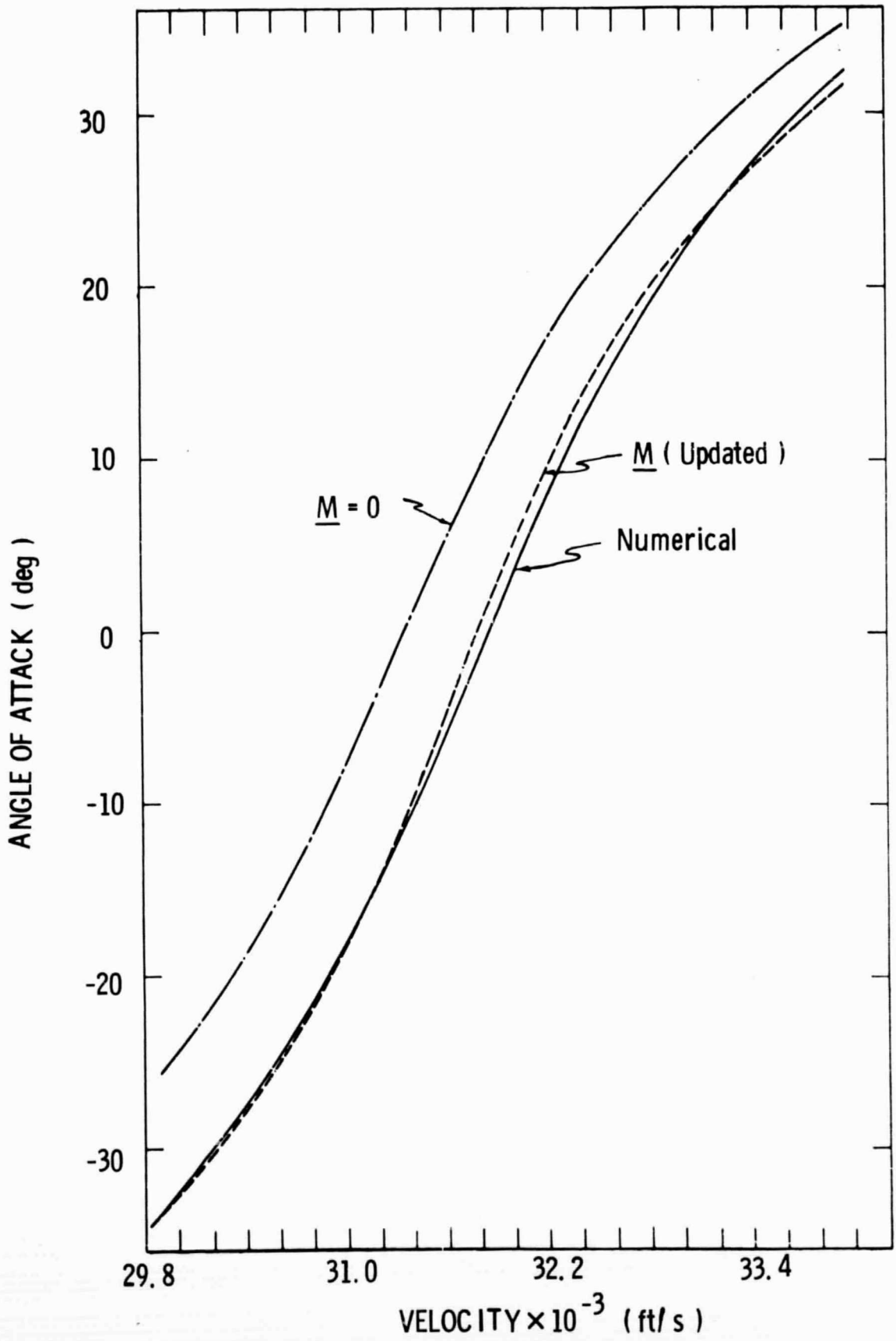

Figure 5 Angle of Attack Versus Velocity

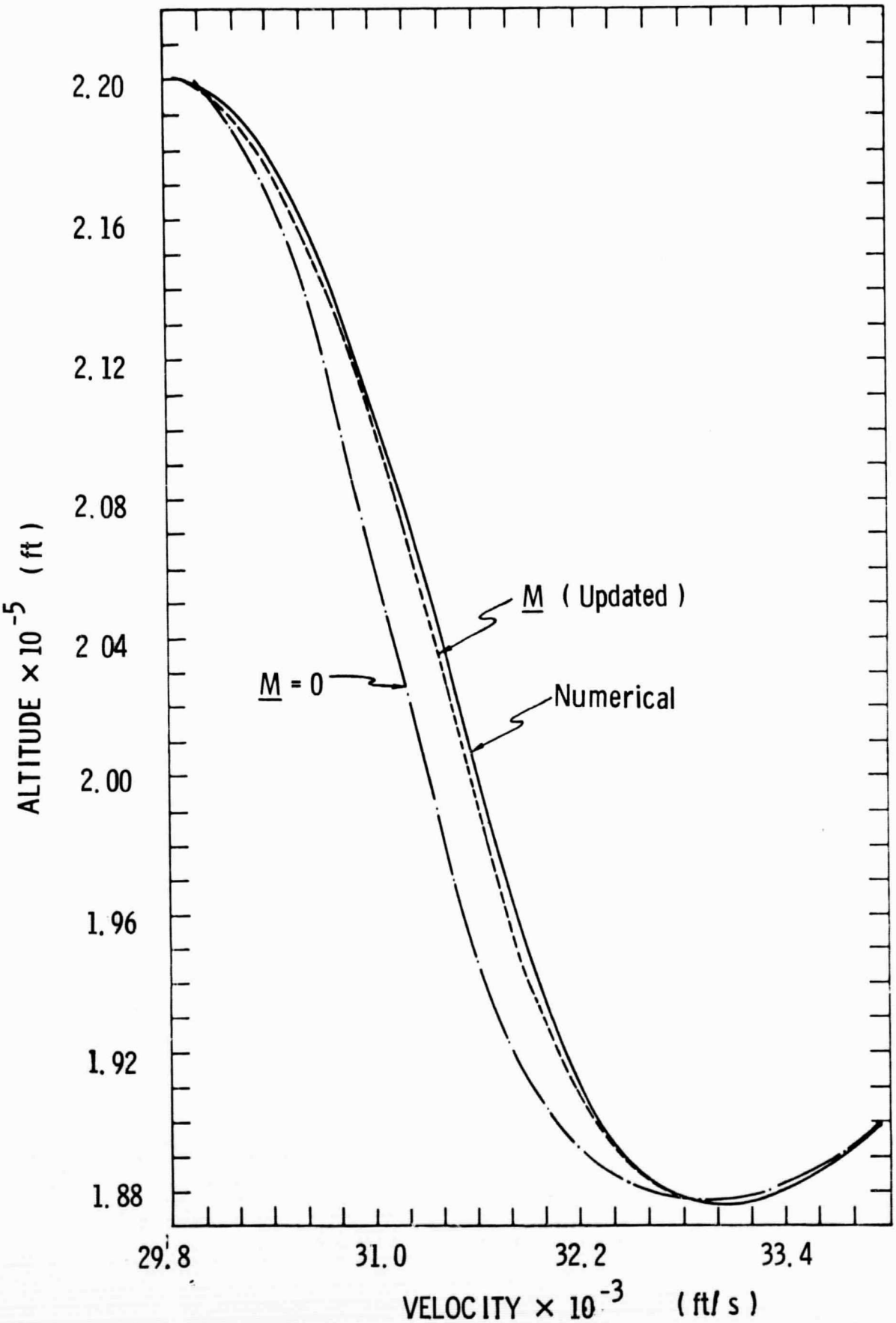

Figure 6 Altitude Versus Velocity

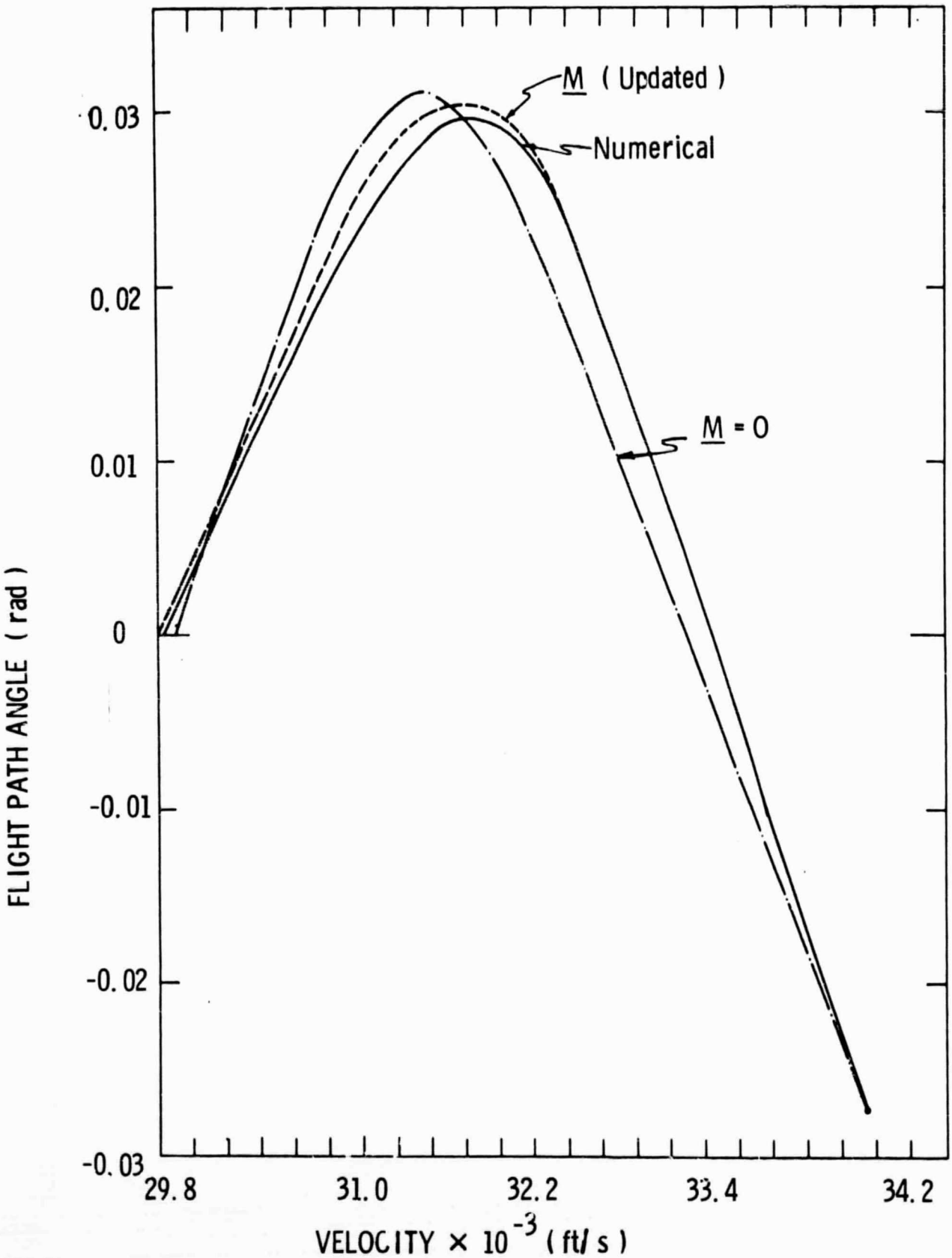

Figure 7 Flight Path Angle Versus Velocity